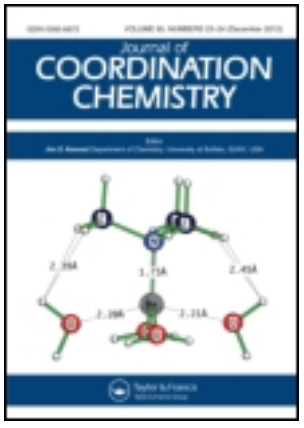

Journal of Coordination Chemistry
Publication details, including instructions for authors and subscription information:
http://www.tandfonline.com/loi/gcoo20

Synthesis, structure, and DNA-binding studies of a dicopper(II) complex with N-phenolato-N′-[2-(dimethylamino) ethyl]oxamide as ligand

Hong-Hua Lu [a], Yan-Tuan Li [a], Zhi-Yong Wu [b], Kang Zheng [a] & Cui-Wei Yan [c]

[a] Marine Drug and Food Institute, Ocean University of China, Qingdao, Shandong 266003, P.R. China

[b] Key Laboratory of Marine Drug, Chinese Ministry of Education, Ocean University of China, Qingdao, P.R. China

[c] College of Marine Life Science, Ocean University of China, Qingdao, Shandong 266003, P.R. China

Published online: 08 Apr 2011.

To cite this article: Hong-Hua Lu, Yan-Tuan Li, Zhi-Yong Wu, Kang Zheng & Cui-Wei Yan (2011) Synthesis, structure, and DNA-binding studies of a dicopper(II) complex with N-phenolato-N′-[2-(dimethylamino) ethyl]oxamide as ligand, Journal of Coordination Chemistry, 64:8, 1360-1374, DOI: 10.1080/00958972.2011.569710

To link to this article: http://dx.doi.org/10.1080/00958972.2011.569710

Journal of Coordination Chemistry
Vol. 64, No. 8, 20 April 2011, 1360–1374

Synthesis, structure, and DNA-binding studies of a dicopper(II) complex with *N*-phenolato-*N*′-[2-(dimethylamino) ethyl]oxamide as ligand

HONG-HUA LU†, YAN-TUAN LI*†, ZHI-YONG WU‡, KANG ZHENG† and CUI-WEI YAN*§

†Marine Drug and Food Institute, Ocean University of China, Qingdao, Shandong 266003, P.R. China
‡Key Laboratory of Marine Drug, Chinese Ministry of Education, Ocean University of China, Qingdao, P.R. China
§College of Marine Life Science, Ocean University of China, Qingdao, Shandong 266003, P.R. China

(*Received 13 December 2010; in final form 22 February 2011*)

A new μ-oxamido-bridged dicopper(II) complex, $[Cu_2(pdmaeox)(bpy)(H_2O)](pic)\cdot H_2O$ [H_3pdmaeox = *N*-phenolato-*N*′-[2-(dimethylamino)ethyl]oxamide, Hpic = 2,4,6-trinitrophenol, bpy = 2,2′-bipyridine], has been synthesized and characterized by elemental analyses, molar conductivity measurement, infrared, and electronic spectra studies, and X-ray single-crystal diffraction. The complex crystallizes in the triclinic system, $P\bar{1}$ space group, with crystallographic data: $a = 10.7815(2)$ Å, $b = 11.3598(2)$ Å, $c = 14.1389(3)$ Å, and $z = 2$. In $[Cu_2(pdmaeox)(bpy)(H_2O)]^+$, one copper(II) resides in the inner site with a square-planar coordination geometry and the other is chelated by the two *exo*-oxygen atoms of the *cis*-pdmaeox^{3-} ligand in a square-pyramidal environment. The Cu···Cu separation through *cis*-pdmaeox^{3-} bridge is 5.1834(4) Å. The crystal structure is stabilized by hydrogen bonds and π–π stacking interactions. The interaction of the dicopper(II) complex with herring sperm-DNA (HS-DNA) has been investigated by electronic absorption titration, fluorescence titration, electrochemical titration, and viscosity measurements. The results reveal that the interaction of the dicopper(II) complex with HS-DNA might be electrostatic binding. The effects of bridging ligand on the interaction of the dinuclear complex with HS-DNA were preliminarily investigated.

Keywords: Crystal structure; Binuclear copper(II) complex; DNA interaction; μ-Oxamido-bridge

1. Introduction

Studies on transition-metal complexes with DNA gain insight into the reactive models for protein–nucleic acid interactions and probes of DNA structure, and get information about drug design and tools of molecular biology [1–6]. Modes of DNA noncovalent interaction with metal complexes include electrostatic effect, groove binding, and

*Corresponding authors. Email: yantuanli@ouc.edu.cn; cuiweiyan@ouc.edu.cn

Journal of Coordination Chemistry
ISSN 0095-8972 print/ISSN 1029-0389 online
DOI: 10.1080/00958972.2011.569710

intercalation; effectiveness mainly depends on the mode and affinity of the binding between the complexes and DNA [7]. As attention has been focused on interactions with DNA [8–11], many copper(II) complexes have been synthesized and their DNA-binding properties studied [12–17], because copper(II) plays an important role in the body, and numerous copper(II) complexes possess anticancer, anticarcinogenic, and antimutagenic effects both *in vitro* and *in vivo* [18]. Relatively few studies on dicopper(II) complexes have been reported [19–22] compared with the number of studies dealing with mononuclear copper(II) complexes. However, the fact that a number of nucleases have two or three metal ions in their catalytic centers [23] stimulated us to design and synthesize new dicopper(II) complexes to get more information about their DNA-binding properties.

N,N′-bis(substituted)oxamides are good candidates as binucleating bridging ligands because their coordinating ability toward transition-metal ions can be modified by changing the amide substituents [24–28]. Compared with extensive research in symmetrical *N,N′*-bis(substituted)oxamide polynuclear systems, only a few dissymmetrical *N,N′*-bis(substituted)oxamide polynuclear complexes have been reported due to the difficulties in their synthesis [29, 30]. However, complexes bridged by dissymmetrical *N,N′*-bis(substituted)oxamides have shown important properties [31–35] prompting us to design and synthesize new polynuclear complexes with dissymmetrical *N,N′*-bis(substituted)oxamides.

In this article, we describe the synthesis and structure of a new μ-oxamido-bridged dicopper(II) complex, $[Cu_2(pdmaeox)(bpy)(H_2O)](pic)\cdot H_2O$, using *N*-phenolato-*N′*-[2-(dimethylamino)ethyl]oxamide (H_3pdmaeox) as a bridging ligand and end-capped with 2,2′-bipyridine (bpy). The DNA-binding properties of the dicopper(II) complex have been studied. To the best of our knowledge, this is the first report about the DNA-binding of the dicopper(II) complex bridged by dissymmetrical *N,N′*-bis(substituted)oxamide containing phenolato group.

2. Experimental

2.1. *Materials*

N-phenolato-*N′*-[2-(dimethylamino)ethyl]oxamide (H_3pdmaeox) was synthesized following the reported method [36]. Ethidium bromide (EB) and herring sperm-DNA (HS-DNA) were purchased from Sigma Corp. and used as received. All other chemicals were of reagent grade and obtained commercially.

2.2. *Synthesis of $[Cu_2(pdmaeox)(bpy)(H_2O)](pic)\cdot H_2O$*

A methanol aqueous solution (5 mL) of copper(II) picrate hexahydrate (0.0627 g, 0.1 mmol) was added dropwise into a methanol solution (5 mL) containing H_3pdmaeox (0.0140 g, 0.05 mmol) and piperidine (0.0128 g, 0.15 mmol). The mixture was stirred quickly for 30 min, then a methanol solution (5 mL) containing 2,2′-bipyridine (0.0078 g, 0.05 mmol) was added slowly. The resulting solution was stirred for 5 h at 333 K. The obtained brown suspension was filtered and the precipitate was recrystallized in a mixture of methanol, water, and acetonitrile (volume ratio

of 1 : 1 : 1). Brown crystals of the dicopper(II) complex suitable for X-ray analysis were obtained from the solution by slow evaporation at room temperature after 3 days. Yield: 65%. Anal. Calcd for $C_{28}H_{28}Cu_2N_8O_{12}$ (%): C, 42.27; H, 3.55; N, 14.08. Found (%): C, 42.24; H, 3.58; N, 14.32.

2.3. *Physical measurements*

Carbon, hydrogen, and nitrogen microanalyses were performed on a Perkin-Elmer 240 elemental analyzer. Molar conductance was measured with a Shanghai DDS-11A conductometer. Infrared (IR) spectra were recorded on a Nicolet-470 spectrophotometer from 4000 to 400 cm^{-1} as KBr pellets. The UV-Vis spectrum was recorded in a 1-cm-path length quartz cell on a Cary 300 spectrophotometer. Fluorescence was tested on an Fp-750w fluorometer. Cyclic voltammetric (CV) experiments were carried out using a CHI 832B electrochemical analyzer with a glassy carbon working electrode (GCE), saturated calomel reference (SCE), and a platinum wire auxiliary electrode.

2.4. *Crystal structure determination*

X-ray diffraction was made on a Bruker APEX area-detector diffractometer with graphite monochromatic Mo-Kα radiation ($\lambda = 0.71073$ Å) at 296 K. The crystal structure was solved by the direct method followed by Fourier syntheses. Structure refinement was performed on F^2 by full-matrix least-squares procedures using SHELXL-97 [37]. Water hydrogens were located in a difference Fourier map and then treated as riding, with $U_{iso}(H) = 1.5U_{eq}(O)$. The remaining hydrogens were placed in calculated positions, with CH = 0.93 Å (aromatic), 0.96 Å (methyl), and 0.97 Å (methylene), and refined in riding mode, with $U_{iso}(H) = 1.2U_{eq}(C)$ for aromatic and methylene groups or $1.5U_{eq}(C)$ for methyl groups. Crystal data of the dicopper(II) complex are summarized in table 1, and selected bond lengths and angles are listed in table 2.

2.5. *DNA-binding studies*

All experiments involving HS-DNA were performed in Tris-HCl buffer solution (pH = 7.19), prepared using deionized and sonicated triply distilled water. A ratio of UV absorbance A_{260}/A_{280} (of 1.95) of the resulting solution was determined at 260 and 280 nm, which indicated the isolation of the DNA from protein [38], and the concentration was determined by UV absorbance at 260 nm, assuming $\lambda_{260} = 6600\ L\ mol^{-1}\ cm^{-1}$ [39]. Stock solution of the DNA was stored at 277 K and was used in no more than 4 days. A concentrated stock solution of the dicopper(II) complex was prepared by dissolving the complex in DMSO and diluting with Tris-HCl buffer to certain concentrations for all the experiments. Absorption spectral titration was performed by keeping the concentration of the dicopper(II) complex constant while varying HS-DNA concentration. An equal volume of HS-DNA was added into the complex solution and reference solution to eliminate the absorbance of the DNA itself. A stock solution of the dicopper(II) complex ($1 \times 10^{-3}\ mol\ L^{-1}$) in Tris-HCl buffer was freshly prepared. The EB Tris-HCl solution (5 μL, 1 mmol L^{-1}) was added to 1 mL of

Table 1. Crystal data and details of the structure determination.

Empirical formula	$C_{28}H_{28}Cu_2N_8O_{12}$
Formula weight	795.66
Temperature (K)	296
Crystal system	Triclinic
Space group	$P\bar{1}$
Unit cell dimensions (Å, °)	
a	10.7815(2)
b	11.3598(2)
c	14.1389(3)
α	87.9970(10)
β	74.3170(10)
γ	68.4820(10)
Volume (Å^3), Z	1547.02(5), 2
Calculated density (g cm^{-3})	1.708
μ(Mo-Kα) (mm^{-1})	1.454
F(000)	812
Crystal size (mm^3)	$0.04 \times 0.06 \times 0.29$
Radiation (Å) (Mo-Kα)	0.71073
Limiting indices	$-13 \le h \le 14$; $-14 \le k \le 14$; $-18 \le l \le 17$
Total, unique data, $R_{(int)}$	13226, 7134, 0.029
θ range (°)	1.93, 27.68
Observed data [$I > 2\sigma(I)$]	4856
R, wR_2, S	0.0411, 0.0888, 1.031
Max., avg shift/error	0.000, 0.000

Table 2. Selected geometric parameters (Å, °).

Cu1–N1	1.919(2)	Cu1–N2	1.922(2)
Cu1–N3	2.010(2)	Cu1–O1	1.9363(18)
Cu2–N4	1.972(2)	Cu2–N5	1.976(2)
Cu2–O2	1.9579(18)	Cu2–O3	1.9613(19)
Cu2–O4	2.273(2)	–	–
N1–Cu1–N2	83.45(9)	N2–Cu1–N3	84.20(9)
O1–Cu1–N1	84.87(8)	N4–Cu2–N5	81.95(10)
N4–Cu2–O4	100.21(9)	N5–Cu2–O4	91.78(9)
O2–Cu2–O3	86.05(8)	O2–Cu2–O4	91.23(8)
O3–Cu2–O4	95.71(8)	–	–

HS-DNA solution (at saturated binding levels) [40] and stored in the dark for 2 h before use. Then the solution of the dicopper(II) complex was titrated into the DNA/EB mixture and diluted in Tris-HCl buffer to 5 mL, producing solutions with varied mole ratio of the dicopper(II) complex to HS-DNA. Before measurements, the mixture was shaken and incubated at room temperature for 30 min. The fluorescence spectra of EB binding to HS-DNA were obtained at an emission wavelength of 584 nm and an excitation wavelength of 522 nm in the fluorometer. CV experiments on the dicopper(II) complex were taken by maintaining constant concentration of the dicopper(II) complex while varying HS-DNA concentration using Tris-HCl buffer solvent. Viscosity measurements were carried out using an Ubbelodhe viscometer immersed in a thermostatic water bath maintained at 289(±0.1) K. HS-DNA samples approximately

200 base pairs in length were prepared by sonication to minimize complexities arising from DNA flexibility [41]. Flow times were measured with a digital stopwatch, and each sample was measured three times to calculate the average flow time. Relative viscosities for HS-DNA in the presence and absence of the dicopper(II) complex were calculated from the equation $\eta = (t - t_0)/t_0$, where t is the observed flow time of the DNA-containing solution and t_0 is that of Tris-HCl buffer alone. Data were presented as $(\eta/\eta_0)^{1/3}$ *versus* binding ratio [42], where η is the viscosity of HS-DNA in the presence of the dicopper(II) complex and η_0 is the viscosity of HS-DNA alone.

3. Results and discussion

3.1. *Synthetic route and general properties of the dicopper(II) complex*

Use of a binucleating bridging ligand that offers both coordination geometry and ligand field strength suitable for metal ions is an effective method for synthesizing dinuclear complexes. In this study, we sought a Cu(II)–Cu(II) dinuclear complex and chose *N*-phenolato-*N*′-[2-(dimethylamino)ethyl]oxamide (H_3pdmaeox) as the bridging ligand. 2,2′-Bipyridine was used as terminal ligand. In preparing the dinuclear complex, piperidine deprotonates H_3pdmaeox for coordination through oxamido nitrogens. In fact, elemental analyses, IR and electronic spectral studies, and single-crystal X-ray diffraction indicate that the reaction of H_3pdmaeox with $Cu(pic)_2 \cdot 6H_2O$ and bpy in 1 : 2 : 1 mole ratio yielded the dinuclear complex $[Cu_2(pdmaeox)(bpy)(H_2O)](pic) \cdot H_2O$, as expected. The dicopper(II) complex is soluble in acetone, DMF, and DMSO giving stable solution and is moderately soluble in water, methanol, and practically insoluble in carbon tetrachloride, chloroform, and benzene at room temperature. In the solid state, the dicopper(II) complex is stable in air allowing physical measurements. The molar conductance of the dicopper(II) complex ($71\,\Omega^{-1}\,cm^{-2}\,mol^{-1}$, in $1 \times 10^{-3}\,mol\,L^{-1}$ DMF solution) falls in the expected range for 1 : 1 electrolytes [43], suggesting that the picrate anion in the complex is outside the coordination sphere. These observations agree with the following IR spectra.

3.2. *IR and electronic spectra*

In order to clarify the mode of bonding, the IR spectrum of the dicopper(II) complex was analyzed in a careful comparison with that of free H_3pdmaeox. The carbonyl (C=O) stretching vibration at $1662\,cm^{-1}$ for the free ligand is red shifted to $1647\,cm^{-1}$ in the dicopper(II) complex, indicating that the oxygens of the carbonyl take part in coordinating to copper(II) [44]. This shift has often been used as a proof of an oxamido-bridge [24]. Bands associated with ν(C=N) and (C=C) of bpy at 1516, 1468, and $1426\,cm^{-1}$ suggest coordinated nitrogen from bpy in the dinuclear complex. Free Hpic has $\nu_s(NO_2)$ at 1344 cm^{-1} and $\nu_{as}(NO_2)$ at $1555\,cm^{-1}$. However, in the dicopper(II) complex, the $\nu_s(NO_2)$ of pic^- at $1344\,cm^{-1}$ splits into two bands at 1316, $1365\,cm^{-1}$, and the $\nu_{as}(NO_2)$ of pic^- emerges at $1565\,cm^{-1}$, suggesting that the nitryl oxygens of pic^- take no part in coordination [45].

In order to obtain further structural information, the electronic spectrum of the complex was recorded in DMF solution, and three absorption bands with varied

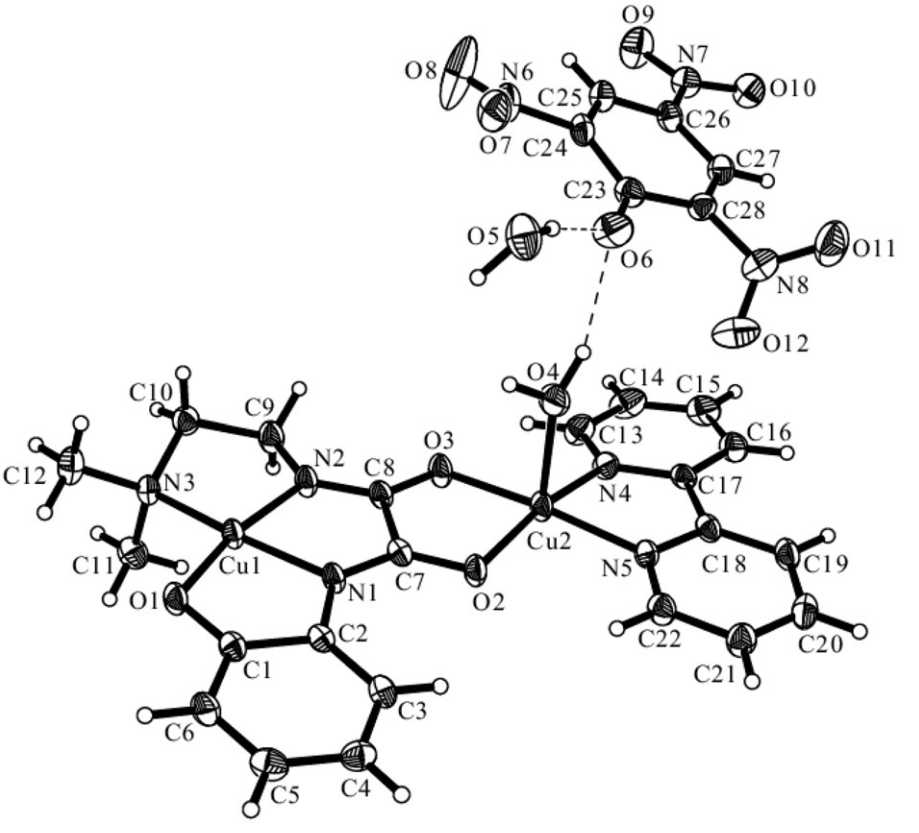

Figure 1. An ORTEP view of the complex with atom-numbering scheme and thermal ellipsoids at 30% probability level. Hydrogens are shown as small spheres of arbitrary radii. Dashed lines show hydrogen bonds.

intensities are observed. The intense band at 242 nm of the dicopper(II) complex is attributed to bpy (π–π*) transition, while the less intense band at 300 nm typical of charge transfer between bpy and metal (ligand-to-metal charge transfer, LMCT). The band at 352 nm corresponds to charge transfer transition between picrate and metal [46].

3.3. *Crystal structure*

The structure of $[Cu_2(pdmaeox)(bpy)(H_2O)](pic)\cdot H_2O$ consists of a dicopper(II) cation $[Cu_2(pdmaeox)(bpy)(H_2O)]^+$, a picrate anion, and a lattice water molecule. An ORTEP of the complex is illustrated in figure 1. Two copper(II) ions are bridged by *cis*-pdmaeox^{3-} with a Cu$\cdots$Cu distance of 5.1834(4) Å. Cu1 at the inner site of pdmaeox^{3-} has a square-planar coordination geometry. The four coordination atoms from pdmaeox^{3-} displace off the plane from 0.0544(10) Å (N3) to 0.0684(12) Å (N1). The five-membered chelate ring Cu1–N2–C9–C10–N3 takes a twist conformation with the puckering parameters [47] of $Q = 0.383(3)$ Å and $\varphi = 121.0(4)^\circ$, while the other two

Table 3. Hydrogen-bonding geometries for the complex (Å, °).

D–H···A	*D*–H	H···A	*D*···A	*D*–H···A
O4–H4A···O1^{i}	0.87	1.97	2.817(3)	167.4
O4–H4B···O6	0.91	2.03	2.899(3)	160.0
O5–H5A···O1^{i}	0.95	2.00	2.926(3)	164.8
O5–H5B···O6	0.91	2.00	2.896(3)	170.9
C21–H21···O10^{ii}	0.93	2.49	3.399(4)	166.6

Symmetry codes: $^{i}-x, -y, 1-z$; $^{ii}x, y, z+1$.

chelate rings are almost planar. Cu2 is located in a square-pyramidal environment with τ of 0.07 [48]. The basal plane is defined by two exo-oxygens of oxamido groups of pdmaeox^{3-} and two nitrogens from bpy, from which the maximum displacement of defined atoms is 0.0362(11) Å for N5. The apical site is occupied by water (O4), by which Cu2 is pulled 0.1623(11) Å out of the basal plane. The stronger donor abilities of the deprotonated amido nitrogens compared to the amino nitrogens [49] show bond lengths of Cu1–N1 [1.919(2) Å] and Cu1–N2 [1.922(2) Å], shorter than that of Cu1–N3 [2.010(2) Å] (table 3). In pic$^-$, three nitros (N6, N7, and N8) twist from the benzene ring plane by 22.5(6)°, 12.6(2)°, and 52.4(3)°, respectively.

In the crystal, two $[Cu_2(pdmaeox)(bpy)(H_2O)]^+$ link through hydrogen bonds between coordination water molecules and phenolic oxygens to form a dimer. These dimers are assembled by pic$^-$ and lattice water molecules into a 1-D chain parallel to the *c*-axis (figure 2). An offset π–π stacking interaction is observed between benzene ring and neighboring pyridine ring containing N5 at $1-x, -y, 1-z$, denoted ^{iii} in figure 3. The centroid–centroid distance is 3.7117(18) Å and the angle of the two ring planes is 4.87(15)°. The smallest separation is 3.299(3) Å for C18^{iii}.

Comparing the crystal structure of $[Cu_2(pdmaeox)(bpy)(H_2O)](pic)\cdot H_2O$ with that of previously reported analog $[Cu_2(oxpn)(bpy)(pic)(H_2O)](pic)$ [50], we find that the two dicopper(II) complexes have the same end-capped ligand (bpy) and counter anion (pic$^-$), and both of them crystallize in triclinic system. The main difference between them is that the bridging ligand in $[Cu_2(pdmaeox)(bpy)(H_2O)](pic)\cdot H_2O$ is *N*-phenolato-*N*′-[2(dimethylamino)ethyl]oxamide (pdmaeox), and in $[Cu_2(oxpn)(bpy)(pic)(H_2O)](pic)$ is *N,N*′-bis(aminopropyl)oxamido (oxpn), which results in the difference of binding mode for pic$^-$. In the present complex, pic$^-$ is only a counter anion, however, in $[Cu_2(oxpn)(bpy)(pic)(H_2O)](pic)$, one pic$^-$ is a counter anion and the other is coordinated. The difference of the binding mode for pic$^-$ in the two dicopper(II) complexes affects DNA-binding properties (*vide infra*).

3.4. *DNA-binding studies*

3.4.1. Electronic absorption titration. Electronic absorption spectroscopy is an effective method to examine binding modes of metal complexes with DNA [51]. In general, the hypochromism and red shift are associated with the binding of metal complexes to the DNA helix, due to intercalation involving a strong stacking interaction between the aromatic chromophore of complexes and the base pairs of

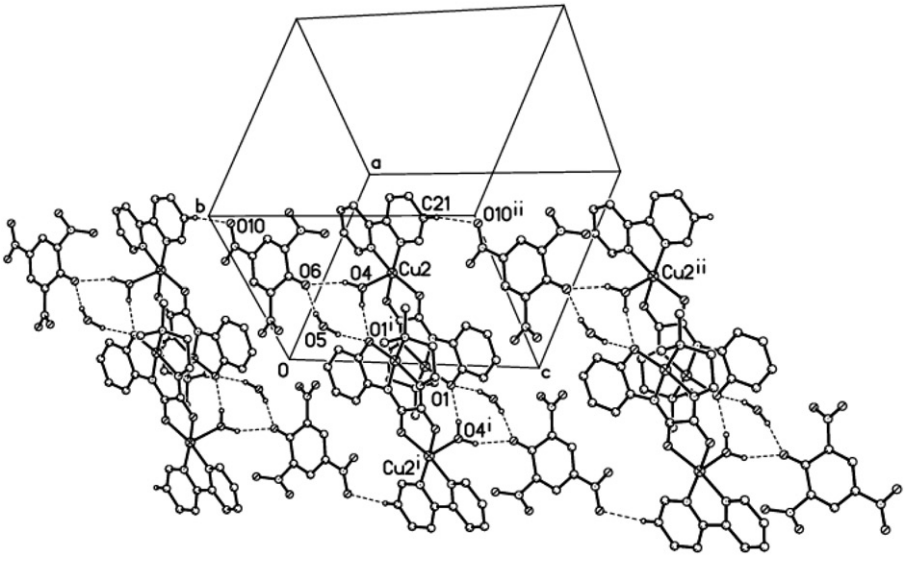

Figure 2. A 1-D hydrogen-bonding structure parallel to the *c*-axis. Hydrogen bonds are shown as dotted lines; hydrogens uninvolved have been omitted for clarity (symmetry codes: [i]$-x, -y, 1-z$; [ii]$x, y, z+1$).

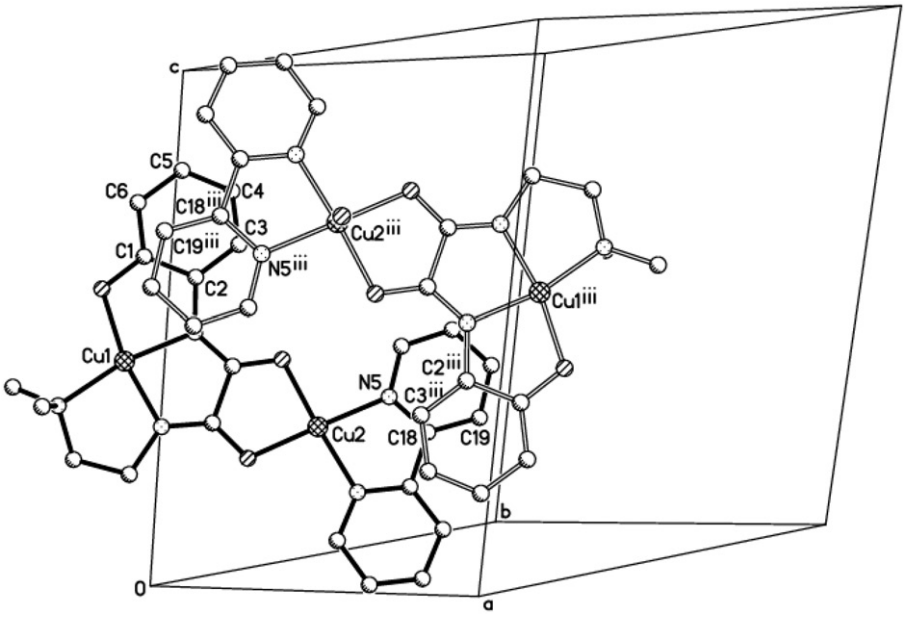

Figure 3. A perspective drawing of π–π stacking interactions in the crystal perpendicular to the plane of benzene ring (symmetry code: [iii]$1-x, -y, 1-z$).

DNA [52]. Absorption spectra of the dicopper(II) complex in the absence and presence of HS-DNA are given in figure 4. When titrated by HS-DNA, the dicopper(II) complex exhibits hypochromic effect and no red shift, implying that the interaction mode between the dicopper(II) complex and HS-DNA might be electrostatic [53].

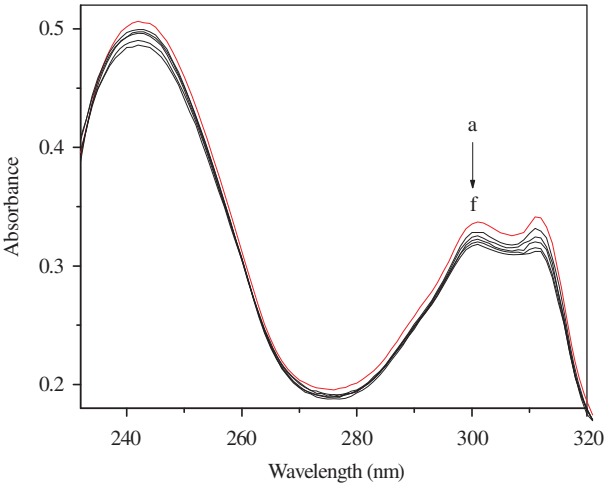

Figure 4. Electronic absorption spectra of the complex in Tris-HCl buffer upon titration of HS-DNA. Arrow indicates the direction of change upon increase of DNA concentration.

To quantitatively evaluate the binding magnitude of the dicopper(II) complex with HS-DNA, the intrinsic binding constant K_b was determined by monitoring changes in absorbance at 300 nm using the following equation [54]:

$$[\mathrm{DNA}]/(\varepsilon_a - \varepsilon_f) = \mathrm{DNA}/(\varepsilon_b - \varepsilon_f) + 1/K_b(\varepsilon_b - \varepsilon_f), \quad (1)$$

where [DNA] is the concentration of DNA, ε_f, ε_a, and ε_b refer to the extinction coefficients for the free complex, for each addition of HS-DNA to the complex and for the complex in the fully bound form, respectively. K_b is estimated to be $3.39 \times 10^4\,(\mathrm{mol\,L^{-1}})^{-1}$ ($R = 0.9977$ for six points) by the ratio of slope to the intercept of the plot of $[\mathrm{DNA}]/(\varepsilon_a - \varepsilon_f)$ *versus* [DNA] (figure 5). The K_b value is lower than those of typical intercalators (e.g., EB-DNA, $\sim 10^6\,(\mathrm{mol\,L^{-1}})^{-1}$) [55] and previously reported tetracopper(II) complex (K_b, $1.47 \times 10^5\,(\mathrm{mol\,L^{-1}})^{-1}$) [56], but higher than that of previously reported electrostatic binding dicopper(II) complex $[Cu_2(heap)(H_2O)_2](pic)_2 \cdot 2H_2O$ (K_b, $2.67 \times 10^4\,(\mathrm{mol\,L^{-1}})^{-1}$) [57]. The effect may be attributed to more π-electrons provided by bpy and aromatic ring in the present complex $[Cu_2(dmaeox)(bpy)(H_2O)](pic) \cdot H_2O$, which increases the affinity of the dicopper(II) complex with HS-DNA.

3.4.2. Fluorescence titration. To further investigate the interaction between dicopper(II) complex and HS-DNA, EB fluorescence displacement experiment was performed, which has been widely used to characterize the interaction of complexes with DNA by following the changes in fluorescence intensity. The intrinsic fluorescence intensity of DNA is low, and that of EB in Tris-HCl buffer is not high due to quenching by solvent. However, the fluorescence intensity of EB can be enhanced on the addition of DNA owing to its intercalation into the DNA. Once the complexes intercalate into DNA, the binding sites of DNA available for EB will be decreased, therefore, the fluorescence intensity of EB-DNA will be quenched [58]. As illustrated in figure 6, the

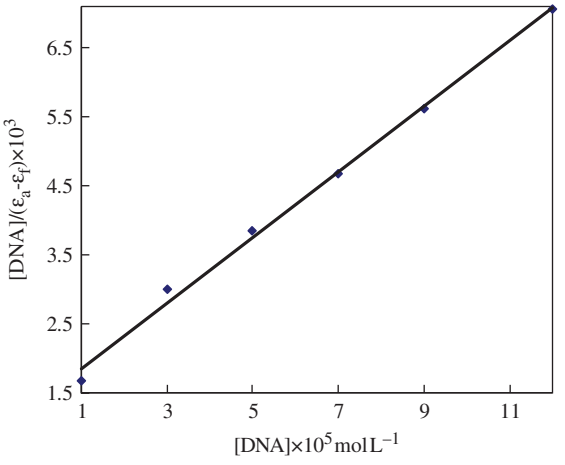

Figure 5. Plot of $[DNA]/(\varepsilon_a - \varepsilon_f)$ *vs.* [DNA] for the absorption titration.

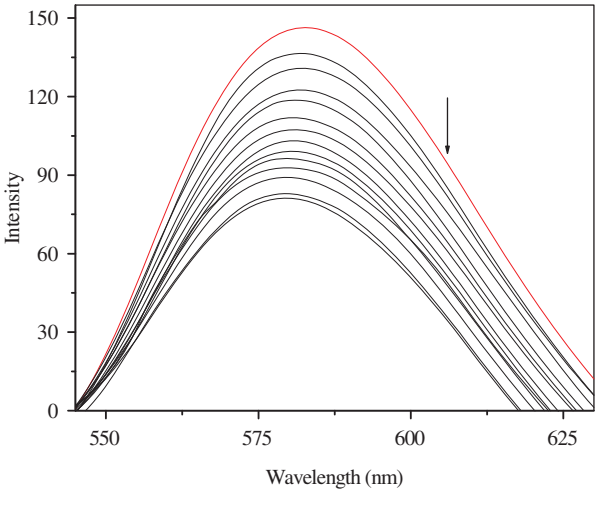

Figure 6. Fluorescence intensity of EB-DNA as the system was titrated with the complex. Arrow shows the direction of change upon increasing the complex concentration.

fluorescence intensity of EB-DNA at 584 nm exhibits a remarkable decrease with increasing concentration of the dicopper(II) complex, suggesting that some EB molecules were released after exchange with the dicopper(II) complex, resulting in fluorescence quenching of EB. The quenching of EB bound to HS-DNA by the dicopper(II) complex is in agreement with the linear Stern–Volmer equation [59]:

$$I_0/I = 1 + K_{sv}[Q], \tag{2}$$

where I_0 and I represent fluorescence intensities in the absence and presence of quencher, respectively. K_{sv} is referred to as the Stern–Volmer constant and $[Q]$ is the

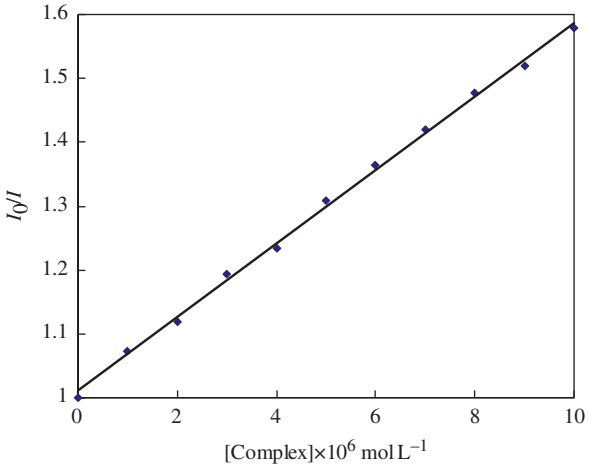

Figure 7. Plot of I_0/I *vs.* [complex] for fluorescence titration.

concentration of quencher. In the quenching plot of I_0/I *versus* [complex] (figure 7), K_{sv} value is given by the ratio of the slope to intercept as 5.69×10^4 ($R = 0.9990$ for 11 points).

3.4.3. Electrochemical titration. CV technique provides a useful complement to the previously used methods of investigating binding of metal complexes to DNA [60]. At a scan rate of 0.24 V s^{-1}, the CV behaviors of the dicopper(II) complex without and with HS-DNA were studied and the results are shown in figure 8. In the absence of HS-DNA (curve a), the dicopper(II) complex exhibits two redox couples corresponding to couple 1: Cu(II)Cu(II)/Cu(II)Cu(I); couple 2: Cu(II)Cu(I)/Cu(I)Cu(I), with the cathodic (E_{pc}) and anodic peak potentials (E_{pa}) being −0.3515 V (E_{pc1}) and −0.0256 V (E_{pa1}), −0.8632 V (E_{pc2}), and −0.5717 V (E_{pa2}), respectively, and one reduction peak at −0.9685 V (E_{pc3}) corresponding to Cu(I)Cu(I)/Cu(I)Cu. The formal potentials of the free dicopper(II) complex ($E_f^{o'}$) are −0.1886 V (couple 1) and −0.7175 V (couple 2). In the presence of HS-DNA (curve b) with $R = 3$ ($R = [DNA]/[complex]$), the peak currents decreased, simultaneously, the cathodic peak potentials (E_{pc}) and the anodic peak potentials (E_{pa}) exhibited significant shifts. The potentials shifted to be −0.3637 V (E_{pc1}) and −0.0552 V (E_{pa1}), −0.8973 V (E_{pc2}), and −0.5915 V (E_{pa2}), and −1.0027 V (E_{pc3}), respectively. The formal potentials of the bound complex ($E_b^{o'}$) (couple 1: −0.2095 V; couple 2: −0.7444 V) shift to more negative potential, indicating interaction may exist between the dicopper(II) complex and HS-DNA.

The shift in the value of the formal potential ($\Delta E^{o'}$) was used to estimate the ratio of equilibrium binding constants K_R/K_O corresponding to the model of interaction described by Bard and Carter [61]:

$$\Delta E^{o'} = E_b^{o'} - E_f^{o'} = 0.059 \log(K_R/K_O), \tag{3}$$

where $E_b^{o'}$ and $E_f^{o'}$ are the formal potentials of the bound and free complexes, respectively, and K_R and K_O are binding constants for reduction and oxidation forms to

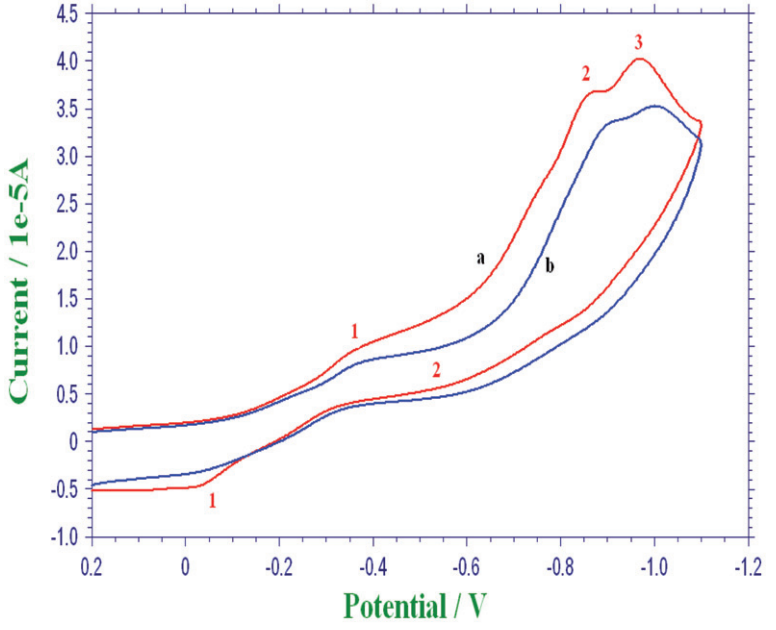

Figure 8. Cyclic voltammograms of the complex in (a) the absence and (b) the presence of DNA with scan rate of $0.24\,V\,s^{-1}$.

HS-DNA, respectively. We calculate $K_{Cu(II)Cu(I)}/K_{Cu(II)Cu(II)}$ and $K_{Cu(I)Cu(I)}/K_{Cu(II)Cu(I)}$ as 0.44 and 0.35, respectively. The results suggest that the Cu(II)Cu(II) form exhibits stronger DNA-binding than the Cu(II)Cu(I) form, and Cu(II)Cu(I) form than Cu(I)Cu(I) form. The present studies lead us to conclude that the dicopper(II) complex may interact with HS-DNA in the mode of electrostatic [62]. It should be pointed out that the Cu(II)Cu(I) species certainly has a lower overall charge than the related Cu(II)Cu(II) but also a very different structure because Cu(I) would be tetrahedral. This would also play a non-negligible role on the proposed electrostatic interaction between DNA and the dicopper(II) unit. Further investigation of these and similar systems is required in order to get a reasonable explanation and deeper insight into the electrochemical titration of metal complexes with DNA.

3.4.4. Viscosity measurement. Due to its sensitivity to change of length of DNA, viscosity determination is regarded as the most effective means to study the binding of complexes to DNA in solution and provides strong arguments for intercalative binding mode [63, 64]. To further confirm the interaction mode of the dicopper(II) complex and HS-DNA, viscosity measurement was carried out. The effects of the dicopper(II) complex on the viscosity of HS-DNA are shown in figure 9. On increasing the amount of the dicopper(II) complex, the relative viscosity of HS-DNA is almost unchanged, consistent with electrostatic binding mode of interaction [65]. Thus, the results obtained from viscosity studies validate those obtained from electronic absorption titration, fluorescence titration, and electrochemical titration.

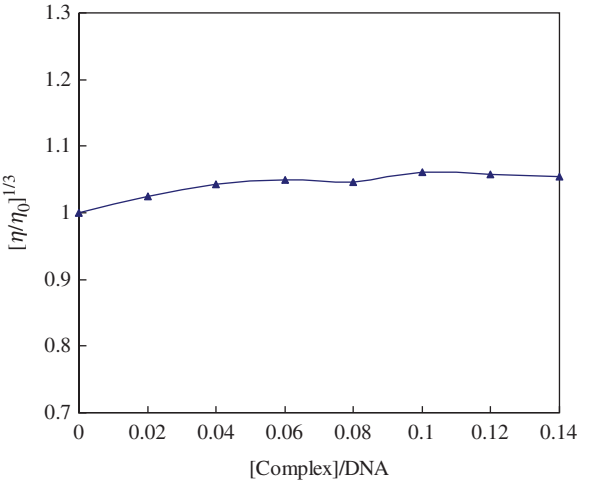

Figure 9. Effect of increasing amount of complex on the relative viscosity of HS-DNA at 289(±0.1) K. [DNA] = 0.1 mmol L^{-1}.

Comparing the DNA-binding property of $[Cu_2(pdmaeox)(bpy)(H_2O)](pic) \cdot H_2O$ with that of $[Cu_2(oxpn)(bpy)(pic)(H_2O)](pic)$ [50], we find that not only the interaction mode but also the DNA-binding ability is different. In the former case the binding mode is electrostatic with the intrinsic binding constant (K_b) of $3.39 \times 10^4 (mol\,L^{-1})^{-1}$, while the latter has intercalation and K_b up to $7.4 \times 10^4 (mol\,L^{-1})^{-1}$. The differences may be attributed to the smaller steric hindrance of the bridging ligand oxpn than that of pdmaeox, which increases the affinity of $[Cu_2(oxpn)(bpy)(pic)(H_2O)](pic)$ with HS-DNA. Further investigations using various bridging ligands are still required in order to confirm this effect and are in progress in our laboratory.

4. Conclusions

The aim of this article is to investigate the interaction of dinuclear complex with DNA. For that, a new μ-oxamido-bridged dicopper(II) complex, $[Cu_2(pdmaeox)(bpy)(H_2O)](pic) \cdot H_2O$, has been synthesized and structurally characterized by single-crystal X-ray diffraction. To the best of our knowledge, this is the first report about DNA-binding of dicopper(II) complex bridged by dissymmetrical *N,N′*-bis(substituted)oxamide containing phenolato group. Furthermore, the interaction of the dicopper(II) complex with HS-DNA has been investigated by electronic absorption titration, fluorescence titration, electrochemical titration, and viscosity measurements. The bridging ligands in dinuclear complexes may influence not only the interaction mode but also the DNA-binding ability. These results confirmed that the interaction of the dinuclear complexes toward HS-DNA may be modified and tuned by changing the bridging ligands. This strategy should be valuable in designing new dinuclear complexes and understanding the binding properties between the complexes and DNA.

Supplementary material

Crystallographic data (excluding structure factors) for the structure reported in this work have been deposited at the Cambridge Crystallographic Data Center and allocated the deposition number CCDC 787066.

Acknowledgments

This project was supported by the National Natural Science Foundation of China (No. 21071133), the Natural Science Foundation of Qingdao City (No. 09-1-3-73-jch), and the Program for Changjiang Scholars and Innovative Research Team in University (IRT0944).

References

[1] M.J. Absalon, W. Wu, J.W. Kozarich, J. Stubbe. *Biochemistry*, **34**, 2076 (1995).
[2] Y. Wang, N. Okabe. *Inorg. Chim. Acta*, **358**, 3407 (2005).
[3] K.E. Erkkila, D.T. Odom, J.K. Barton. *Chem. Rev.*, **99**, 2777 (1999).
[4] H.T. Chifotides, K.R. Dunbar. *Acc. Chem. Res.*, **38**, 146 (2005).
[5] V. Rajendiran, R. Karthik, M. Palaniandavar, H. Stoeckli-Evans, V.S. Periasamy, M.A. Akbarsha, B.S. Srinag, H. Krishnamurthy. *Inorg. Chem.*, **46**, 8208 (2007).
[6] E.R. Jamieson, S.J. Lippard. *Chem. Rev.*, **99**, 2467 (1999).
[7] B.A. Chabner, T.G. Roberts. *Nat. Rev. Cancer*, **5**, 65 (2005).
[8] H. Rauter, R.D. Domenico, E. Menta, A. Oliva, Y. Qu, N. Farrell. *Inorg. Chem.*, **36**, 3919 (1997).
[9] Y. Qu, A. Harris, A. Hegmans, A. Petz, P. Kabolizadeh, H. Penazova, N. Farrell. *J. Inorg. Biochem.*, **98**, 1591 (2004).
[10] B.D. Wang, Z.Y. Yang, T.R. Li. *Bioorg. Med. Chem.*, **14**, 6012 (2006).
[11] H. Zhang, C.S. Liu, X.H. Bu, M. Yang. *J. Inorg. Biochem.*, **99**, 1119 (2005).
[12] B.K. Santra, P.A.N. Reddy, G. Neelakanta, S. Mahadevan, M. Nethaji, A.R. Chakravarty. *J. Inorg. Biochem.*, **89**, 191 (2002).
[13] S. Mahadevan, M. Palaniandavar. *Inorg. Chim. Acta*, **254**, 291 (1997).
[14] F. Liu, K.A. Meadows, D.R. McMillin. *J. Am. Chem. Soc.*, **115**, 6699 (1993).
[15] R. Tamilarasan, D.R. McMillin. *Inorg. Chem.*, **29**, 2798 (1990).
[16] D.S. Sigman, T.W. Bruice, A. Mazumder, C.L. Sutton. *Acc. Chem. Res.*, **26**, 98 (1993).
[17] S. Mahadevan, M. Palaniandavar. *Inorg. Chem.*, **37**, 693 (1998).
[18] J.R.J. Sorenson (Ed.). *Biology of Copper Complexes*, Humana Press, Clifton, NJ (1987).
[19] J.Z. Wu, L. Yuan, J.F. Wu. *J. Inorg. Biochem.*, **99**, 2211 (2005).
[20] F. Zhang, Q.Q. Zhang, W.G. Wang, X.L. Wang. *J. Photochem. Photobiol. A: Chem.*, **184**, 241 (2006).
[21] Y.P. Li, Y.B. Wu, J. Zhao, P. Yang. *J. Inorg. Biochem.*, **101**, 283 (2007).
[22] Q.Q. Zhang, F. Zhang, W.G. Wang, X.L. Wang. *J. Inorg. Biochem.*, **100**, 1344 (2006).
[23] W.N. Lipscomb, N. Sträter. *Chem. Rev.*, **96**, 2375 (1996).
[24] H. Ojima, K. Nonoyama. *Coord. Chem. Rev.*, **92**, 85 (1988).
[25] R. Ruiz, J. Faus, F. Lloret, M. Julve, Y. Journaux. *Coord. Chem. Rev.*, **193–195**, 1069 (1999).
[26] E. Pardo, R. Ruiz-García, J. Cano, X. Ottenwaelder, R. Lescouëzec, Y. Journaux, F. Lloret, M. Julve. *J. Chem. Soc., Dalton Trans.*, 2780 (2008).
[27] M.C. Dul, E. Pardo, R. Lescouëzec, Y. Journaux, J. Ferrando-Soria, R. Ruiz-García, J. Cano, M. Julve, F. Lloret, D. Cangussu, C.L.M. Pereira, H.O. Stumpf, J. Pasán, C. Ruiz-Pérez. *Coord. Chem. Rev.*, **254**, 2281 (2010).
[28] M.G. Rodríguez, V.M.J. Pérez, J.E.H. Rivera, J.M. Domínguez, R. Contreras, R. Quijada. *Polyhedron*, **26**, 4321 (2007).
[29] S.Q. Zang, R.J. Tao, Q.L. Wang, N.H. Hu, Y.X. Cheng, J.Y. Niu, D.Z. Liao. *Inorg. Chem.*, **42**, 761 (2003).
[30] Z.D. Matović, V.D. Miletić, G. Samardžić, G. Pelosi, S. Ianelli, S. Trifunović. *Inorg. Chim. Acta*, **358**, 3135 (2005).

[31] J.P. Costes, F. Dahan, A. Dupuis, J.P. Laurent. *Inorg. Chem.*, **39**, 169 (2000).
[32] K. Jitsukawa, H. Takahashi, R. Hyuga, H. Arii, H. Masuda. *Eur. J. Inorg. Chem.*, 4140 (2004).
[33] J. Larionova, S.A. Chavan, J.V. Yakhmi, A.G. Froystein, J. Sletten, C. Sourisseau, O. Kahn. *Inorg. Chem.*, **36**, 6374 (1997).
[34] Y. Pei, O. Kahn, K. Nakatani, E. Codjovi, C. Mathonière, J. Sletten. *J. Am. Chem. Soc.*, **113**, 6558 (1991).
[35] Y. Pei, K. Nakatani, O. Kahn, J. Sletten, J.P. Renard. *Inorg. Chem.*, **28**, 3170 (1989).
[36] B.M. Ji, Z.X. Zhou, K.L. Ding, Y.Z. Li. *Polyhedron*, **17**, 4327 (1998).
[37] G.M. Sheldrick. *SHELXL-97*, *Program for Crystal Structure Refinement*, University of Göttingen, Germany (1997).
[38] J. Marmur. *J. Mol. Biol.*, **3**, 208 (1961).
[39] M.E. Reichmann, S.A. Rice, C.A. Thomas, P. Doty. *J. Am. Chem. Soc.*, **76**, 3047 (1954).
[40] J.K. Barton, J.M. Goldberg, C.V. Kumar, N.J. Turro. *J. Am. Chem. Soc.*, **108**, 2081 (1986).
[41] J.B. Chaires, N. Dattagupta, D.M. Crothers. *Biochemistry*, **21**, 3933 (1982).
[42] G. Cohen, H. Eisenberg. *Biopolymers*, **8**, 45 (1969).
[43] W.J. Geary. *Coord. Chem. Rev.*, **7**, 81 (1971).
[44] K. Nakamoto. *Infrared and Raman Spectra of Inorganic and Coordination Compounds*, 5th Edn, Wiley, New York (1997).
[45] S.X. Liu, W.S. Liu, M.Y. Tan, K.B. Yu. *J. Coord. Chem.*, **39**, 105 (1996).
[46] M. Bourgoin, K.H. Wong, J.Y. Hui, J. Smid. *J. Am. Chem. Soc.*, **97**, 3462 (1975).
[47] D. Cremer, J.A. Pople. *J. Am. Chem. Soc.*, **97**, 1354 (1975).
[48] A.W. Addison, T.N. Rao, J. Reedijk, J. Van Rijin, G.C. Verschoor. *J. Chem. Soc., Dalton Trans.*, 1349 (1984).
[49] C. Jubert, A. Mohamadou, C. Gérard, S. Brandes, A. Tabard, J.P. Barbier. *J. Chem. Soc., Dalton Trans.*, 2660 (2002).
[50] Y.L. Song, Y.T. Li, Z.Y. Wu. *J. Inorg. Biochem.*, **102**, 1691 (2008).
[51] A. Wolfe, G.H. Shimer Jr, T. Meehan. *Biochemistry*, **26**, 6392 (1987).
[52] V.A. Bloomfield, D.M. Crothers, I. Tinoco. *Physical Chemistry of Nucleic Acids*, p. 432, Harper and Row, New York (1974).
[53] R. Vijayalakshmi, M. Kanthimathi, V. Subramanian, B.U. Nair. *Biochem. Biophys. Acta*, **1475**, 157 (2000).
[54] A.M. Pyle, J.P. Rehmann, R. Meshoyrer, C.V. Kumar, N.J. Turro, J.K. Barton. *J. Am. Chem. Soc.*, **111**, 3051 (1989).
[55] J.B. Lepecq, C. Paoletti. *J. Mol. Biol.*, **27**, 87 (1967).
[56] X.W. Li, M. Jiang, Y.T. Li, Z.Y. Wu, C.W. Yan. *J. Coord. Chem.*, **63**, 1582 (2010).
[57] X.W. Zhang, Y.J. Zheng, Y.T. Li, Z.Y. Wu, C.W. Yan. *J. Coord. Chem.*, **63**, 2985 (2010).
[58] R. Indumathy, S. Radhika, M. Kanthimathi, T. Weyhermuller, B.U. Nair. *J. Inorg. Biochem.*, **101**, 434 (2007).
[59] O. Stern, M. Volmer. *Z. Phys.*, **20**, 183 (1919).
[60] S. Mahadevan, M. Palaniandavar. *Inorg. Chem.*, **37**, 693 (1998).
[61] M.T. Carter, M. Rodriguez, A.J. Bard. *J. Am. Chem. Soc.*, **111**, 8901 (1989).
[62] P.T. Selvi, M. Palaniandavar. *Inorg. Chim. Acta*, **337**, 420 (2002).
[63] L. Fin, P. Yang. *J. Inorg. Biochem.*, **68**, 79 (1997).
[64] S. Satyanarayana, J.C. Dabrowiak, J.B. Chaires. *Biochemistry*, **31**, 9319 (1992).
[65] C.W. Jiang, H. Chao, H. Li, L.N. Ji. *J. Inorg. Biochem.*, **93**, 247 (2003).